Biophysical Chemistry 6 (1977) 321–335

POLYAMINES–SICKLING RED BLOOD CELL INTERACTION *

Paul W. CHUN **, Eugene E. SAFFEN, Richard J. DiTORE, Owen M. RENNERT and Neil H. WEINSTEIN

Departments of Biochemistry and Molecular Biology, Pediatrics and Medicine, Colleges of Arts and Sciences and Medicine, University of Florida, Gainesville, Florida 32610, USA

Received 23 August 1976
Revised manuscript received 10 December 1976

The binding of polyamine as a function of concentration to normal and sickling red blood cells is analyzed by Langmuir type binding isotherms, based on the Gouy–Chapman model for an electrical double layer, where the zeta potential is a function of only the normal distance coordinate. For normal erythrocytes, the apparent exotropic binding constants are found to be 103, 110, and 130 dl/g at normal distance coordinates of 4, 5, and 6 Å, respectively. The esotropic binding constant is determined to be 420 dl/g at a distance of 7 Å. For sickling red blood cells, the apparent exotropic binding constants are 3.3, 3.8, 4.6, and 6.7 dl/g at a distance of 4 to 7 Å. The esotropic binding constant at a distance of 8 Å is found to be 12.9 dl/g. The apparent binding affinity of polyamines to the normal red blood cell, therefore, is approximately 30 times greater than to the sickling erythrocyte.

The Praxis pulse nuclear magnetic resonance spectrometer is used to determine the spin–lattice relaxation time (T_1) for water in the presence of normal and sickling red blood cells. The spin–lattice relaxation time is found to be 540 ms for normal erythrocytes and 445 ms for sickling red blood cells in the oxy state. Differences in the spin–spin relaxation time (T_2) for the two types of erythrocyte are negligible, being within the range of normal experimental error.

1. Introduction

A great deal of data on the surface alteration and deformation of the red blood cell has been obtained by examining the electrokinetic behavior of its electrical double layer [1–5], rheological flow behavior [8–11], recognition and binding isotherms of a variety of external chemical substances to the surface receptors of the erythrocytes [12–15], fluorescence labeling to reduce the negative surface charge [16,17], and electron micrographic examination of sickled red blood cells under deoxy conditions [15].

Under physiological conditions, the red blood cell has a negative electrical surface charge, the magnitude and distribution of which affects its interaction with any other surface or ligand molecule. The electrokinetic properties or surface charge densities of the erythrocyte may be evaluated based on the electrical double layer theory [2,18,19], knowing that the presence of an electrical charge at the red blood cell membrane in contact with a ligand will influence the ionic distribution within the system.

Although a meaningful relationship between the electrokinetic charge density and the zeta potential of the red blood cell may be formulated using the Gouy–Chapman equation, a lack of knowledge of the detailed molecular architecture of the peripheral zone precludes the application of a more refined theory for surface charge density calculation.

Heard and Seaman [20] have demonstrated that surface charge densities for human red blood cells, calculated from their experimental data, could fit an adsorption isotherm of the Langmuir type.

Polyamine analysis in bone samples of leukemic and nonleukemic conditions has revealed increased concentrations of putrescine, spermidine, and

* This work was supported by National Science Foundation Grant BMS 71-00850-A03 and PCM76-04367 and in part, by General Research Support, College of Medicine, University of Florida. We are grateful for the assistance provided by the University of Florida Computer Center.
** Address all correspondence to Dr. P.W. Chun, Department of Biochemistry and Molecular Biology, College of Medicine, Box J 245, JHMHC, University of Florida, Gainesville, Florida 32610, USA.

spermine in proliferating cells [21–25], and elevation and alteration of the polyamine content of blood in the inherited disorder, cystic fibrosis [26,27].

Variations in their distribution patterns indicate that spermidine and spermine may fulfil different functions in the human body [28]. It has been determined, however, that ornithine decarboxylase is the controlling enzyme in the pathway of polyamine biosynthesis [21,22]. Induction of ornithine decarboxylase and the concentration of polyamines are closely linked to cellular proliferation, with a potential relationship existing between polyamines as a "third messenger" and cyclic nucleotide metabolism.

We have previously reported a notable elevation in the polyamine content of sickling red blood cells when compared to that of the normal erythrocyte. Measurement of the zeta potentials of the two types of erythrocytes in 1.5% glycine buffer, pH 7.4, reveals a surface charge density variation in the red blood cell membrane which may account, in part, for the observed variation in polyamine binding [29–33].

A great deal of nuclear magnetic resonance data for biological systems has appeared in the literature, including some work which compares normal and sickling red blood cells [34–37]. Researchers have reported differences in relaxation rates and accounted for these differences in terms of a change in the mobility of water molecules bound to hemoglobin molecules.

In most NMR experiments, the technique consists of slowly sweeping the radio frequency applied to a sample in a fixed magnetic field, the rapid sweep rate of either frequency or magnetic field between certain limits, and free procession of short pulses of radio frequency at discrete intervals.

This pulse method has proven to be the most versatile for measuring T_1, the spin–lattice relaxation time, or net relaxation of the proton to the preferred orientation, i.e., ground level, after the radio frequency (rf) is applied, i.e., spin flipping or longitudinal relaxation time. At equilibrium, nuclei are distributed among the energy levels according to the Boltzman distribution. After the application of rf energy, the nuclear spin system returns to equilibrium with its lattice by a first-order relaxation process [28,29].

To account for processes that cause nuclear spins of the water to come to equilibrium with each other, the spin–spin relaxation time, T_2, can be measured by application of low radio frequency energy. T_2 is generally related to a lorentzian line shape, with a line of full width at half maximum intensity [38,39].

In this communication, we report on a comparison of the spin–lattice relaxation times (T_1) and spin–spin relaxation times (T_2) of water in a solution of packed normal and sickling erythrocytes. The use of red blood cell surface charge potential variation (ψ_0) as a function of polyamine concentration is proposed to evaluate the apparent exotropic and esotropic binding constants, K_{app}^{ex} and K_{app}^{es}, to determine the magnitude of the interaction between polyamines and normal or sickling red blood cells. Esotropic interaction of polyamines *in vivo* results in perturbation of the Stern layer as a result of electrostatic or hydrophobic bonding, or conjugation with the red blood cell membrane, as differentiated from exotropic interaction in which there is little alteration of the Stern layer.

2. Materials and methods

2.1. Isolation of red blood cells

Ten to fifteen milliliters each of whole blood from donors with normal and homozygous sickling hemoglobin were collected in Heparin tubes and centrifuged at 900 r.p.m. in an HN-S centrifuge (International, a division of Damon) for 20 minutes prior to decanting the serum and leukocytes. The cells were washed eight times in 10 ml of isotonic 0.9% NaCl solution and centrifuged for 20 minutes at 1000 r.p.m. after each washing. A greater degree of adhesion was observed for the sickling red blood cell in solution during this washing procedure. All subsequent procedural operations were completed during a two-day period. Prolonged standing for greater lengths of time at 4°C resulted in a leaching of hemoglobin from the cells. Hematocrit values for red blood cells from sickle cell anemia patients were 18–30, as compared with 40–45 for erythrocytes from normal donors.

2.2. Electrophoretic mobility of red blood cells

The electrophoretic mobility of the red blood cell is measured in 1.5% glycine buffer, pH 7.4, as a function of polyamine concentration with a Riddick

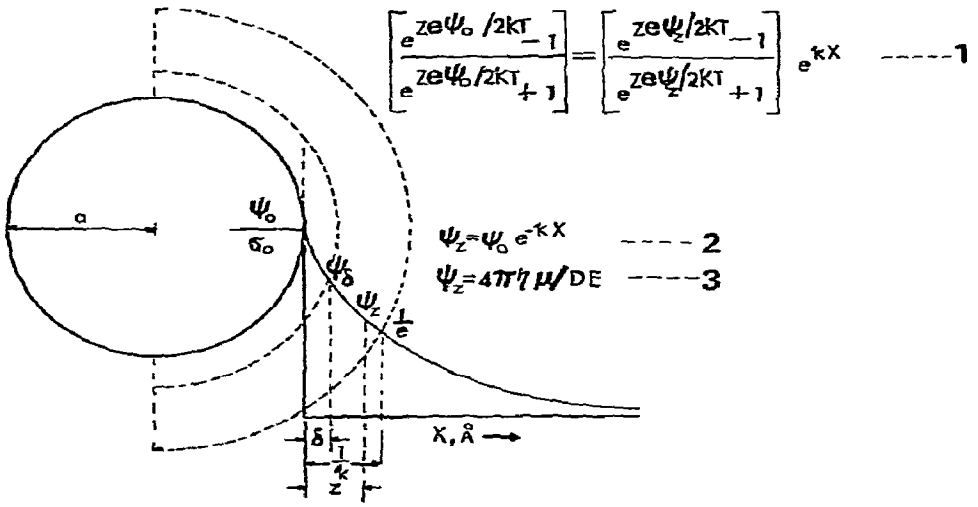

Fig. 1. Gouy–Chapman model for evaluation of surface potential of the electrical double layer. Eq. (3) is the Helmholtz–Smoluchowski equation, where D is the dielectric constant, μ is the electrophoretic mobility of the red blood cell, and η is the viscosity of the medium in poises. ψ_δ = Stern potential. δ, Z, and $1/k$ are Stern, zeta, and Debye–Hückel distances, respectively. The zeta potential lies between $1/k$, which is 37% of exponential, and δ. x, in Å, is varied toward the cell surface from the shearing plane where ψ_Z is measured.

Zeta Meter (Zeta Meter, Inc., New York). The electrophoretic mobility was computed from the current intensity, dimensions of the cell, and the specific conductance of the solution, using the Helmholtz–Smoluchowski equation [18].

The zeta potential was also measured as a function of concentration of polyamine and $CaCl_2$ (from 10–1000 nmole/ml). The concentration of red blood cells in suspension was diluted to an equivalent to 1×10^{-4} M/heme for each sample, using the ratio of molar extinction of 576 to 541 nm of 1.066. The original concentration of washed red blood cells was approximately 1×10^9 cells/ml.

2.3. Analysis of polyamine

One ml of Heparinized blood or washed red blood cells was extracted with an equal volume of 10% sulfosalicylic acid. The mixture was stirred for a few minutes and then centrifuged at 8000 r.p.m. for 20 minutes. Extraction was repeated twice. The supernatant was lyophilized and resuspended in 0.5 ml of 0.2 N sodium citrate buffer, pH 2.2, and then filtered through a millipore filtration apparatus. Polyamine content was determined using the Durrum D-500 high-pressure chromatographic analyzer coupled with a digital data PDP/M coupler.

2.4. Analysis of polyamine binding isotherms

The surface charge density (σ_0) of the univalent electrolytes of the flat electrical double layer is treated according to Verwey and Overbeek [18], where the zeta potential (ψ_z) within the double layer is a function of only the normal distance coordinate x (in Å). Gouy–Chapman's model for evaluation of ψ_0 takes the form of eq. (1), shown in fig. 1, where $y = Ze\psi_z/KT$ and $y_0 = Ze\psi_0/KT$. Z is the valence of the ions, e is the charge of electron, K denotes the Boltzman constant, and $1/k$ is the Debye–Hückel length (in Å). In those cases where $y_0 \ll 25.7$ mV, eq. (1) is reduced to eq. (2) of fig. 1. Eq. (3) is used for determination of the zeta potential, ψ_z, measured at 22°C.

(i) The first method of examining polyamine binding to the red blood cell (Rbc + polyamines $\rightleftharpoons$ Rbc : polyamines) is based on the Langmuir-type of linear binding isotherm shown below:

$1/\psi_0 = 1/\psi_m K_a C + 1/\psi_m$,

where $\psi_0 = \psi_m e^{kx}$ is the electrical potential at the surface of the red blood cell, ψ_m is the zeta potential measured after polyamine binding, C is the concentration of polyamines, and $K_{app}^{ex/es}$ is the apparent binding constant of polyamine to the red blood cell as a function of the normal distance coordinate x, plotting $1/\psi_0$ versus $1/C$.

(ii) The second method of analysis is based on a Langmuir-type expression, except that the fraction of red blood cells bound with polyamine is measured, plotting $1/(\psi_m^0 - \psi_z^0)$ versus $1/C$.

$1/(\psi_m^0 - \psi_z^0) = -1/K_a \psi_z^0 C - 1/\psi_z^0$,

where $\psi_z = -52$ mV and -45 mV for normal and sickling erythrocytes, respectively. ψ_z^0 is the zeta potential at zero concentration of polyamine, which is equivalent to the total zeta potential of the red blood cells. ψ_m^0 is the zeta potential of the unbound red blood cells after the addition of polyamines. Thus, the fraction of the zeta potential influenced by polyamine binding to the red blood cell is: $(\psi_z^0 - \psi_m^0)/\psi_z^0$.

2.5. Preparation of fluorescein conjugated to polyamine

Fluorescein conjugated polyamines were prepared from fluorescein isothiocyanate (FITC, Difco): 100 mg of spermidine in 7 ml of carbonate-buffered saline, pH 9.5, was added to 0.25 mg FITC in 1 ml acetone and incubated for 30 minutes at room temperature. Polyamine–FITC was purified by reprecipitation in the cold and gel filteration on Sephadex G-25 [16,17].

The washed red blood cells were incubated with fluorescein conjugated polyamines in BSG buffer, 291 osmolality (16.24 g NaCl, 2.45 g Na_2HPO_4, 0.44 g $NaH_2PO_4 \cdot H_2O$, 4.03 g dextrose) for two hours at 37°C.

2.6. Isolation and preparation of red blood cells for T_1 and T_2 measurement

Twenty to thirty milliliters each of whole blood from several donors with normal and homozygous sickling hemoglobin were collected in Heparin tubes and the red blood cells prepared as described previously.

A second set of samples similarly prepared were then washed in 0.9% NaCl in D_2O solution (obtained from Isotopic Products, 99.7% D, No. MD75, Merck, Sharp, and Dohme, Canada Limited Co., Montreal, Canada).

The washed cells in either 0.9% NaCl in H_2O or D_2O were packed into quartz G-S tubes specially designed for pulse nuclear magnetic resonance studies, measuring 7.5 cm by 1 cm in diameter. The cells were tightly packed and centrifuged at 800 r.p.m. until no further sedimentation occurred. Centrifugation was continued for approximately 30 minutes until all extraneous water that was not tightly bound to the red blood cells had been removed. At this point, the maximum hematocrit value of 74–75% is reached.

All subsequent Praxis pulse nuclear magnetic resonance studies of the resulting solution were completed within one day. Prolonged standing for greater lengths of time at 4°C resulted in a leaching of hemoglobin from the cells.

2.7. Measurement of T_1

T_1 was measured using a Praxis pulse NMR spectrometer (PR103, 10 MHz), with a 90°–90° program. Provided $T_1 \gg T_2$, the free induction following the first 90° pulse decays to zero more rapidly than the magnetization along the z axis reaches its equilibrium value, M_0. Hence, a second 90° pulse permits a sampling of M_z at a variable delay time, τ. The magnetization rapidly decreases to a steady state value dependent on τ and T_1. When $M_z = 0$ at $t = 0$, the Bloch plot [38] becomes $\ln(A_\infty - A_\tau)$ versus τ, giving a straight line from which T_1 can be determined from the slope. A_τ is the initial amplitude of the free induction decay following the 90° pulse at time τ, and A_∞ is the limiting value of the amplitude at τ for a very long interval between the 90° and 90° pulse.

2.8. Measurement of T_2

The spin–spin relaxation time, T_2, was measured using a 90°–180° pulse program similar to Hahn's procedure [39], providing for the application of a 90°–τ–180° sequence and the observation at a time

2τ of a free induction "echo". The net magnetization along the z axis, M_z, is the vector sum of individual microscopic magnetizations, M_i, arising from nuclei in different parts of the sample and, hence, experiencing slightly different values of the applied field. M_0 loses coherency along M_x, and each M_i decreases in magnitude during transverse relaxation in the time T_2. Thus, echo amplitude depends on T_2, and this quantity may in principle be determined from a plot of peak echo amplitude as a function of τ. It is necessary to carry out a separate pulse sequence for each value of τ and to wait between sequences an adequate time for restoration of equilibrium.

A 60 MHz nuclear magnetic resonance spectrometer was also used to determine the chemical shift of water in normal and sickling red blood cells. Results were compared with those from a Praxis pulse NMR spectrometer.

3. Results

3.1. Surface potential variation as a function of polyamine concentration

We previously reported that the spermidine content of whole blood from 24 patients with sickle cell anemia was approximately ten times greater than that of whole blood from normal donors: 35.97 ± 17.9 nmole/ml as compared to 3.87 ± 1.29 nmole/ml from normal donors. For spermine, the difference is three-fold: 13.52 ± 5.41 nmole/ml as compared to 4.01 ± 1.37 nmole/ml from normal donors [29–34].

The quantity of spermidine and spermine present in sickling samples is five to six times that of the normal red blood cells. The polyamine contents of erythrocytes from donors with different forms of hemoglobinopathies are compared with those of normal red blood cells in table 1. In every case, the spermidine content of these abnormal erythrocytes was higher than that of the normal red blood cells. In some instances, we also noted a considerable elevation of the putrescine content. No differences were observed, however, in the polyamine content of normal red blood cells and the erythrocytes of cystic fibrosis patients.

At the physiological pH 7.4 in glycine buffer, the zeta potential of normal red blood cells is about −52 mV (−3.6 $\mu m\ s^{-1}\ V^{-1}$ cm), whereas that of sickling erythrocytes is −45 mV (−3.4 $\mu m\ s^{-1}\ V^{-1}$ cm). In 5% sucrose solution at pH 7.4, the zeta potential of the normal erythrocyte is −19 mV (−1.2 $\mu m\ s^{-1}$

Table 1
Polyamine content of erythrocytes (nmole/10^9 cell)

	Putrescine	Spermidine	Spermine
Normal AA Rbc (N = 9)	0.007	1.39 ± 0.46	0.9 ± 0.27
Normal AA Rbc (prosthetic heart valve with hemolysis) (N = 1)	0.009	1.64	1.20
Sickle SS Rbc (N = 3)	0.01	6.81 ± 6.40	6.95 ± 6.30
(N = 1) [a]	15.1	40.8	4.29
HbAC Rbc [b] (N = 1)	0.005	3.91	0.6
HbSA Rbc [b] (N = 2)	trace	0.94 ± 0.42	1.64 ± 0.31
HbSC Rbc [c] (N = 2)	6.73 ± 1.26	5.11 ± 1.37	0.47 ± 0.24
Cystic fibrosis Rbc [c] (N = 4)	trace	1.55 ± 0.25	0.99 ± 0.27

[a] Leukocyte count of this donor was twice as high as that of other homozygous sickle cell patients examined. Hematocrit value of 18%.
[b] Sample had a hematocrit value of 45%.
[c] Sample had a hematocrit value of 34%.

V^{-1} cm), as compared with –26 mV (–2.0 μm s^{-1} V^{-1} cm) in 5% sorbitol.

Our measurements also show that the increase in zeta potential (ψ_z) as a function of pH is slow and gradual for red blood cells in sucrose or sorbitol, with a maximum zeta potential of –38 mV (–2.8 μm s^{-1} V^{-1} cm) at pH 10.2 and –45 mV (–3.4 μm s^{-1} V^{-1} cm) at pH 10.0. Such a gradual shift in zeta potential makes it extremely difficult to determine the surface charge density distribution (σ_0) from the Gouy–Chapman equation [2,18–20]. The Gouy–Chapman equation for univalent electrolytes used in these computations, expressed in stat coulomb/cm^2, is

$$\sigma_0 = 2(NKT/2000\pi)^{1/2}(DI)^{1/2}\sinh(e\psi_0/2KT),$$

where K is the Boltzmann constant, N is Avogadro's number, T is the temperature in K, D is the dielectric constant of glycine buffer (89.9), I is the ionic strength of buffer (0.126), e denotes the charge of electron, and σ_0 is the surface charge potential.

The surface charge potential (ψ_0) variation of normal and sickling red blood cells was computed based on the Debye–Hückel exponential model, $\psi_z = \psi_0 e^{-kx}$, and the Gouy–Chapman model for an electrical double layer [18] given by eq. (1) as shown in fig. 1, where Z is the valence of the ions. The zeta potential lies between $1/k$, the Debye–Hückel length, which is 37% of exponential, and δ, the thickness of the Stern layer. x, in Å, is varied toward the cell surface from the shearing plane where ψ_z is measured.

As seen in fig. 2, the surface charge density variations (ψ_0) for the normal erythrocyte from the Debye–Hückel exponential model were determined to be –23.8, –28.6, –34.7, –43.0, –54.4, and -70.4×10^3 stat coulomb/cm^2 at normal distance coordinates of 3, 4, 5, 6, 7, and 8 Å, respectively. Based on the Gouy–Chapman model, we calculated the surface charge variations for the normal red blood cell, shown in fig. 3, to be –27.9, –38.0, –58.4, –122.8, and -1421.9×10^3 stat coulomb/cm^2 at normal distance coordinates of 3, 4, 5, 6, and 7 Å, respectively, as compared to –21.2, –26.9, –36.2, –54.3, –106.0,

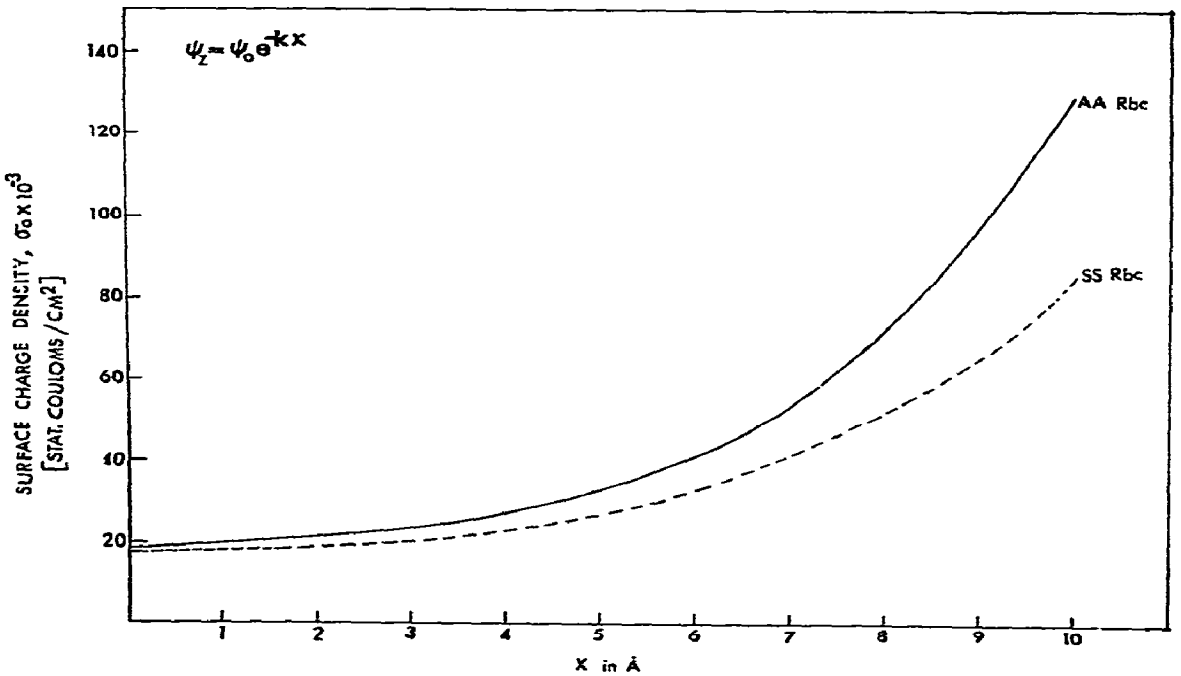

Fig. 2. Plot of surface charge density variation of the Gouy–Chapman model based on the Debye–Hückel exponential function, ψ_0, as a function of the normal distance coordinate, x, in Å, for normal (AA) and sickling (SS) red blood cells (dotted line).

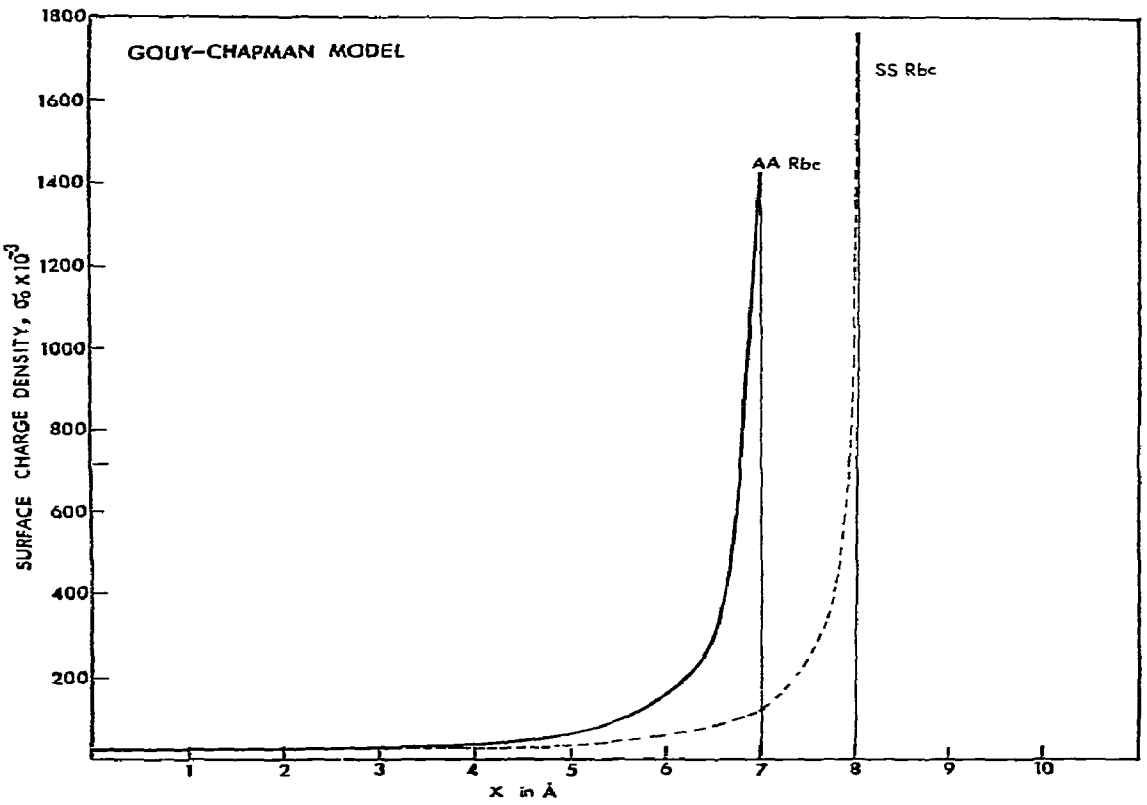

Fig. 3. Plot of surface charge density variation of the Gouy–Chapman model as a function of the normal distance coordinate, x, in Å, for normal (AA) and sickling (SS) red blood cells. Graph has been truncated close to the surface (7 Å for AA, 8 Å for SS, dotted line), since surface charge density decreases beyond these distances.

and -1765.3×10^3 stat coulomb/cm^2 for sickling erythrocytes at 3 to 8 Å.

3.2. *Polyamine binding isotherms*

Fig. 4 shows a computer plot of $1/\psi_0 e^{-\kappa x}$ versus $1/C$, the polyamine concentration, for normal and sickling erythrocytes. The non-linearity of the plot indicates that multiple independent binding sites are probably present in the normal and sickling red blood cells. The limited binding of polyamines to the sickling red blood cells, at normal distance coordinates of 3 to 8 Å, which is apparent in the hyperbolic curves, is consistent with the change in zeta potential of only 7 mV. The sigmoidal curves exhibited for the normal red blood cell, at various distance coordinates, strongly indicate that polyamine binding may be biphasic, that is, both esotropic and exotropic in nature.

In plotting Gouy–Chapman's surface potential, $1/(\psi_m^0 - \psi_2^0)$, versus the concentration of spermidine, $1/C$, for normal and sickling red blood cells, the biphasic nature of polyamine binding becomes apparent in both cases, as may be seen in figs. 4 and 5.

The apparent exotropic binding constants of polyamine with the sickling erythrocytes are 3.3, 3.8, 4.6, and 6.7 dl/g at x distances of 4 to 7 Å, respectively. The esotropic binding constant is 12.9 dl/g at 8 Å (see fig. 5). The surface charge density variations of the sickling red blood cells, prior to the addition of polyamine, were found to be -26.9, -36.2, -54.3, -106, and -1765×10^3 stat coulomb/cm^2 at normal distance coordinates of 4 to 8 Å.

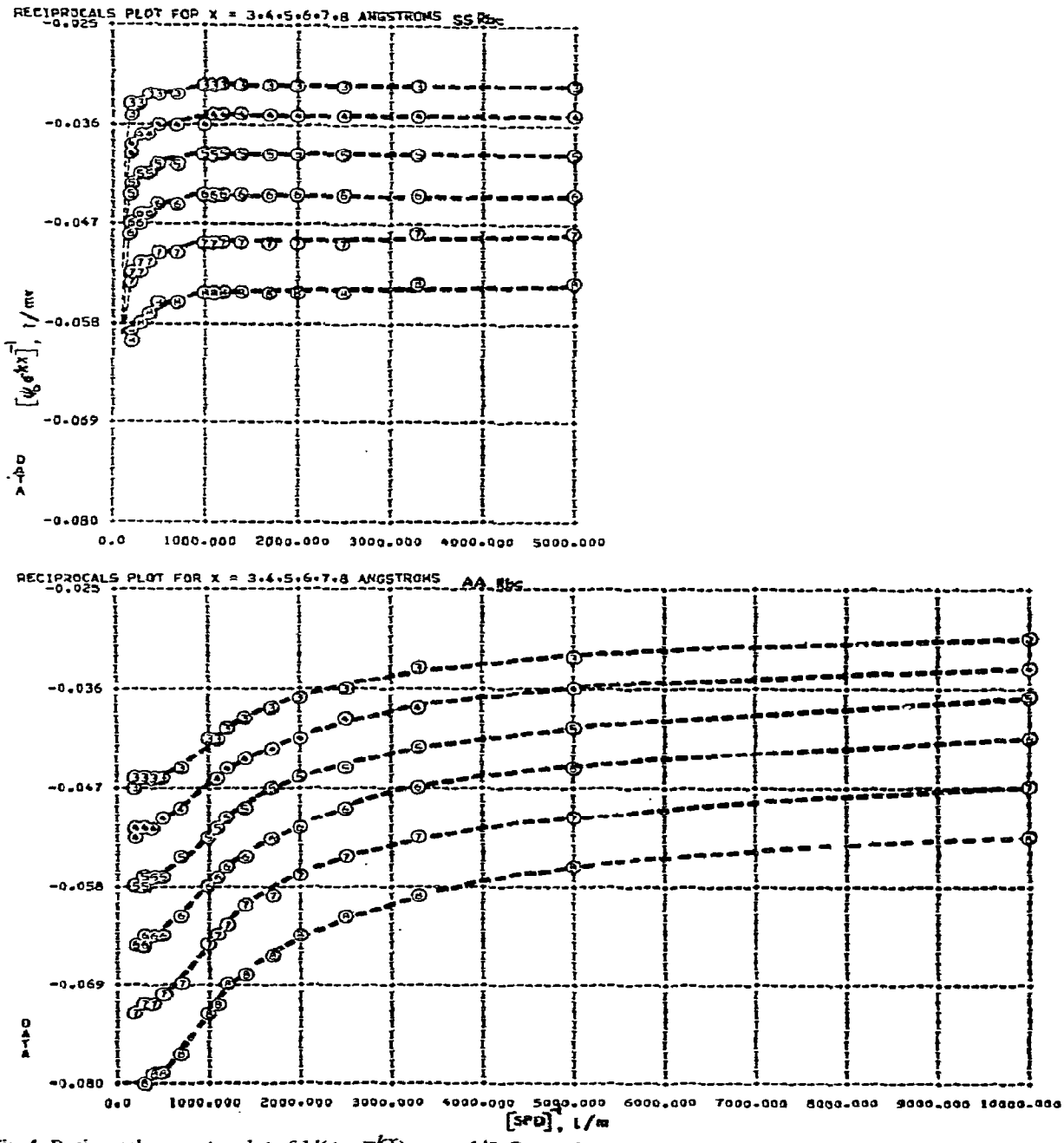

Fig. 4. Reciprocal computer plot of $1/(\psi_0 e^{-kx})$ versus 1/SPD, as a function of spermidine concentration, for sickling (SS) and normal (AA) red blood cells. $\psi_z = \psi_0 e^{-kx}$, where ψ_z is the measured zeta potential and ψ_0 is the surface charge potential calculated as a function of the normal distance coordinate, x, in Å, toward the cell surface from the shearing plane. Zeta potential values are an average of ten measurements for each of several red blood cell samples. Circle with number represents the normal distance coordinate, x, in Å. This plot was obtained by applying the first method of examining polyamine binding described in the text.

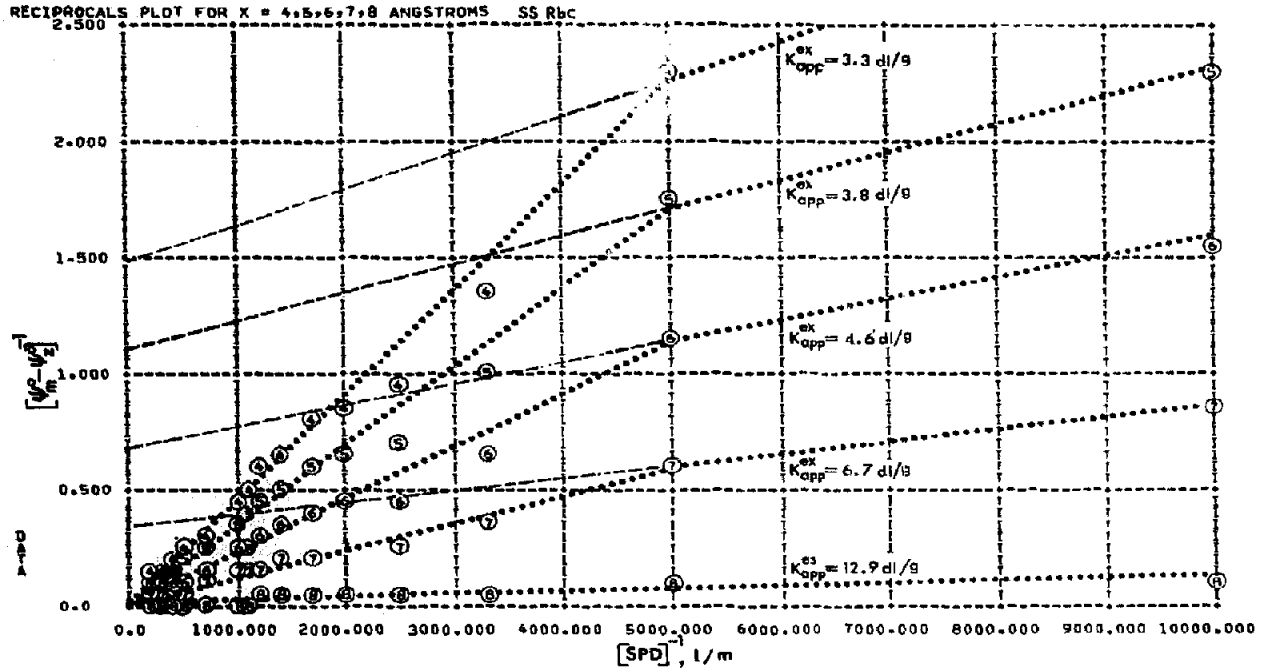

Fig. 5. Reciprocal computer plot of $1/(\psi_m^0 - \psi_z^0)$ versus 1/SPD for sickling red blood cells. ψ_m^0 values are computed from Gouy–Chapman's model, based on eq. 1 in fig. 1, varying the normal distance coordinate from 4 A to 8 A toward the cell surface from the shearing plane. This plot was obtained by applying the second method of analysis described in the text.

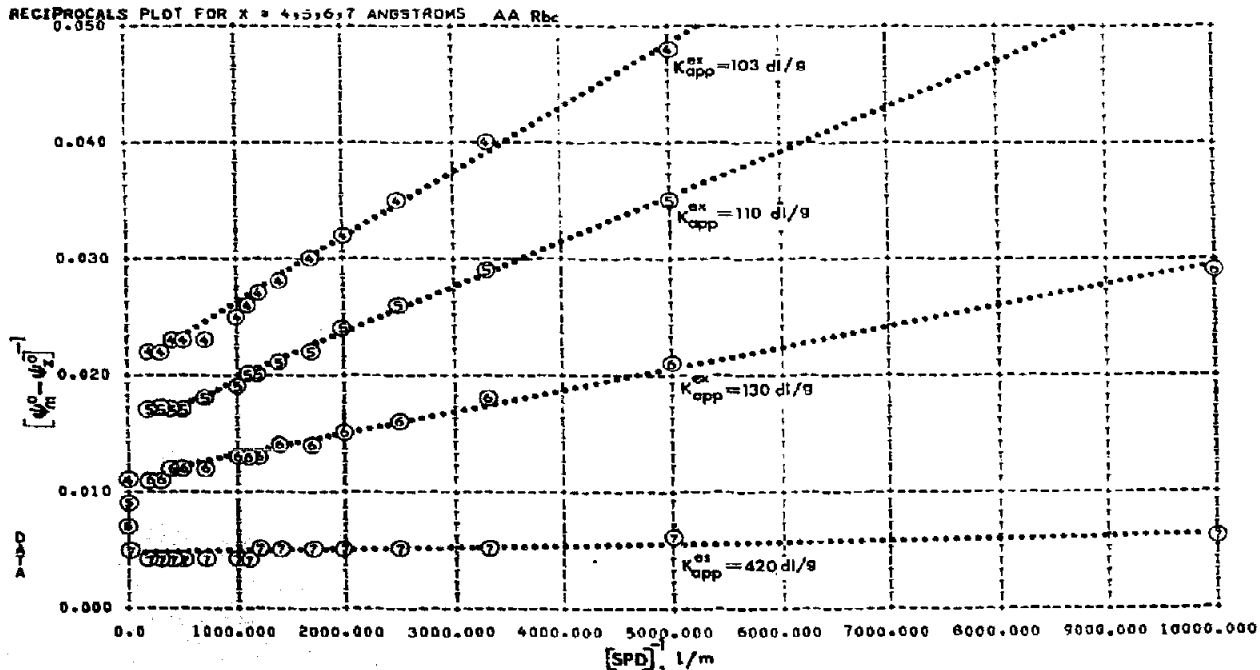

Fig. 6. Reciprocal computer plot of $1/(\psi_m^0 - \psi_z^0)$ versus 1(SPD) for normal red blood cells, varying the normal distance coordinate from 4 A to 7 A. This plot was obtained by applying the second method of analysis described in the text.

As seen in fig. 6, the apparent exotropic binding constants of polyamine with normal red blood cells are 103, 110, and 130 dl/g at normal distance coordinates of 4 to 6 Å, while the esotropic binding constant was found to be 420 dl/g at 7 Å. The surface charge density variations of the normal erythrocytes were determined to be −38.0, −58.4, −122.8, and -1421.9×10^3 stat coulomb/cm^2 at normal distance coordinates of 4 to 7 Å.

From our results, we would surmise that the electrical double layer of the sickling red blood cell is 1 Å thicker than that of the normal red blood cell. Assuming that the zeta potential of the normal red blood cell is −52 mV in 1.5% glycine buffer at pH 7.4, then the electrical double layer field would be 3.2×10^6 V/cm, with $(\psi_0 - \psi_z) = -225$ mV, and the thickness of the electrical double layer being 7 Å. For sickling erythrocytes with a zeta potential of −45 mV at pH 7.4, this measurement would be 3.0×10^6 V/cm, where $(\psi_0 - \psi_z) = -234$ mV, and the electrical double layer is 8 Å thick. The length of the Debye–Hückel layer is estimated to be 9.16 Å in both cases.

3.3. Pulse nuclear magnetic resonance spectra of red blood cells

The chemical shift of water in both normal and sickling red blood cells measured by 60 MHz nuclear magnetic resonance spectrometer was approximately 5.3 δ (ppm), as shown in figs. 7A and 7B. The same chemical shifts were obtained for samples washed with D_2O, as seen in figs. 8A and 8B. The nuclear magnetic resonance spectra were integrated and the spin–spin relaxation time, T_2, was determined from the full line width at half maximum intensity. The results were found to be 45 ms ± 8% in both cases.

In D_2O, additional peaks which may be attributed to the membrane were observed at 1.9 δ and 3.4 δ. Integation of these peaks showed no difference in the normal and sickling red blood cell samples.

Fig. 9 shows a plot of the pulse echo reading versus a delay time which varied from 8 to 30 ms for measurement of the spin–spin relaxation time, T_2, in normal and sickling red blood cell samples in H_2O. No differences were observed within the range of experimental error.

However, measurements of the spin–lattice relaxation time, T_1, shown in fig. 10, revealed that T_1 for the sickling red blood cell sample in H_2O was approximately 100 ms less than T_1 for normal erythrocytes. A similar experiment was attempted in D_2O. However, due to the limitations of the instrument, no detectable signal was obtained. When cells were not packed to a maximum hematocrit value of 74%, however, this variation in T_1 for the two types of erythrocyte was not observed.

3.4. Fluorescein–polyamine conjugate interaction with the red blood cell

Distribution of the binding sites on the surface of red blood cells into clusters or into highly polarized aggregates or patches is induced by interaction with fluorescein–spermidine as shown in fig. 11, resulting in adsorptions and eventually formation of holes as has been observed previously [16,17,40]. Interaction of fluorescein–spermidine with surface negative charges leads primarily to formation of electrostatic bonds whereby reduction of repulsive potential occurs. As seen from this photograph (fig. 11), the clustering and merging of labelled polyamine presumably results from random movements of surface bound components of the red blood cells. The redistribution of surface bound labelled polyamine results in patches distinctly visible throughout the surface of the membrane, with high binding affinity ($2–3 \times 10^6$ polyamine molecules/red blood cell).

4. Discussion

If polyamines are absorbed on the red blood cell by electrostatic attraction alone, then the surface charge density, σ_0, should be equivalent to the Gouy–Chapman calculations of the same value. Under the experimental conditions studied, ψ_δ, the Stern layer, should change very little since the absorption surface density of the polyamines should be directly proportional to the square root of the concentration of added polyamines.

Our studies indicate, however, that in sickling red blood cells the thickness of the electrical double layer increases by 1 Å, measuring 8 Å, as compared with 7 Å for the normal red blood cell. This suggests that polyamines *in vivo* will strongly interact in the

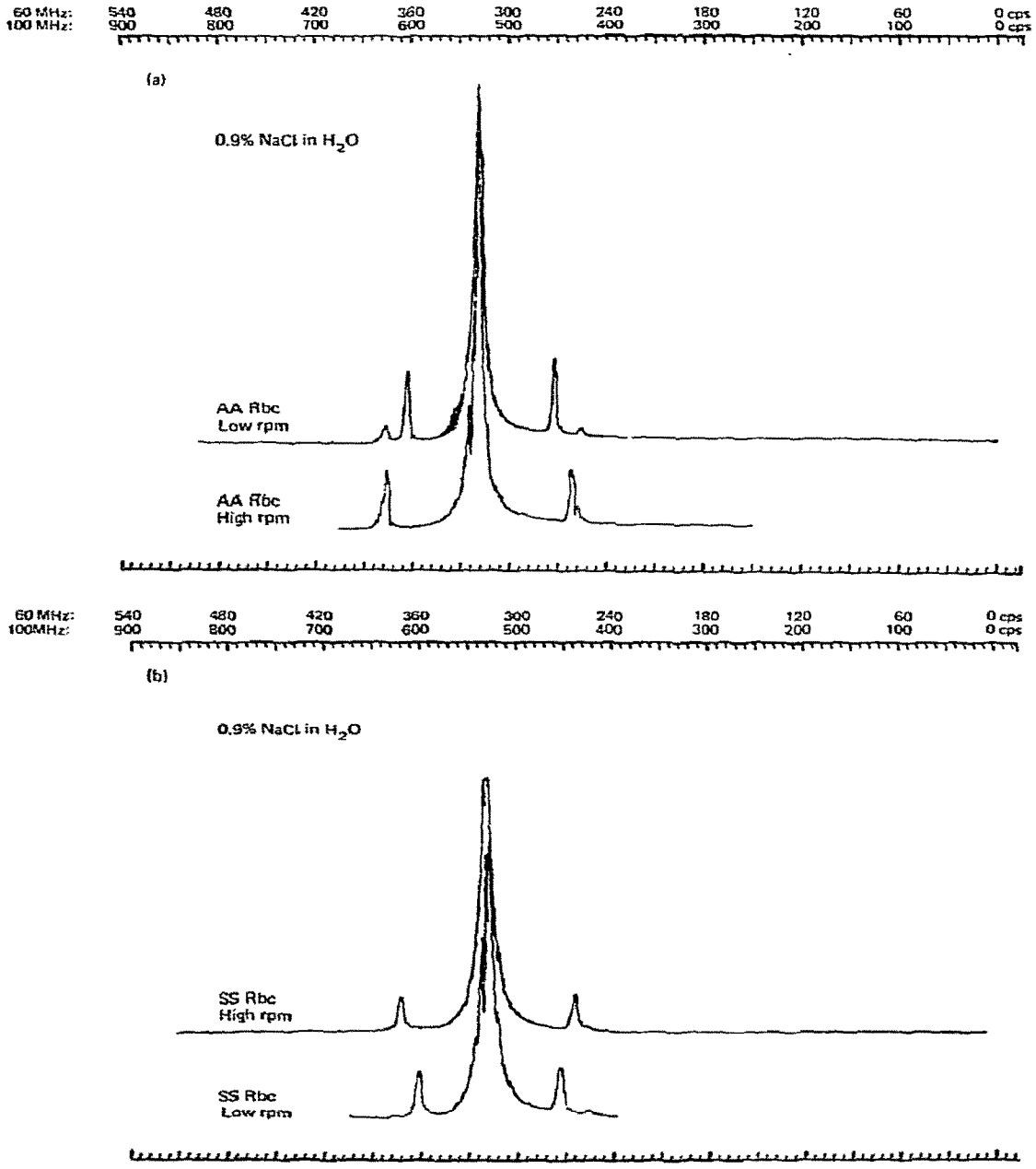

Fig. 7. Chemical shift of H_2O in red blood cells (washed with 0.9% NaCl in H_2O) measured by 60 MHz nuclear magnetic resonance spectrometer, as compared with tetramethylsilane, $Si(CH_3)_4$, standard, 0 δ. (A) normal AA red blood cells, chemical shift of H_2O at 5.3 δ at high and low r.p.m. (B) Sickling SS red blood cells, chemical shift of H_2O at 5.3 δ at high and low r.p.m.

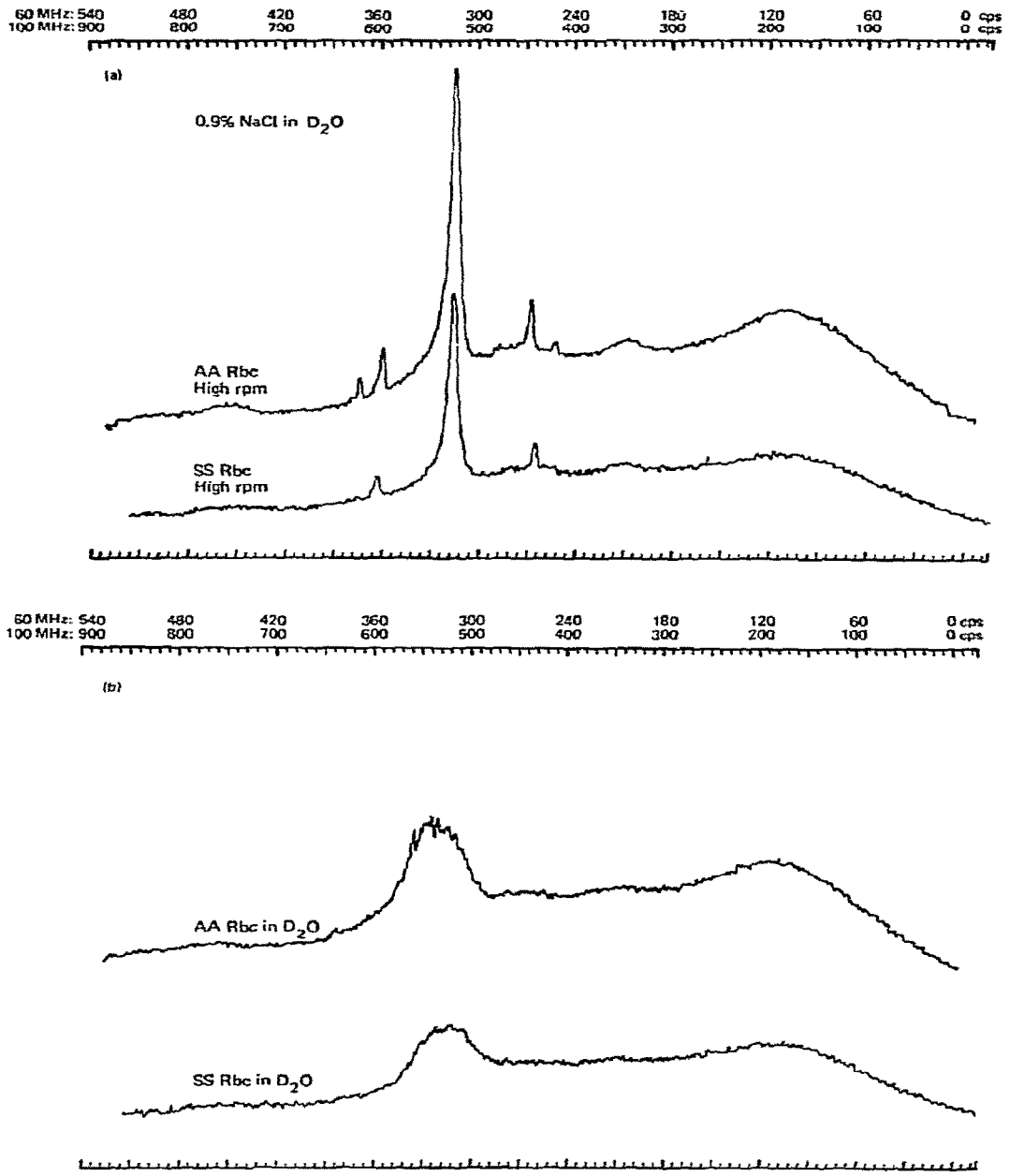

Fig. 8. Chemical shift of H_2O in red blood cells (washed with 0.9% NaCl in D_2O) measured by 60 MHz nuclear magnetic resonance spectrometer, as compared with tetramethylsilane standard, 0 δ. (A) Normal AA red blood cells, chemical shift of H_2O at 5.3, at high r.p.m. (B) Normal AA and SS red blood cells both showing chemical shift of H_2O at 5.3 δ, without spinning the sample.

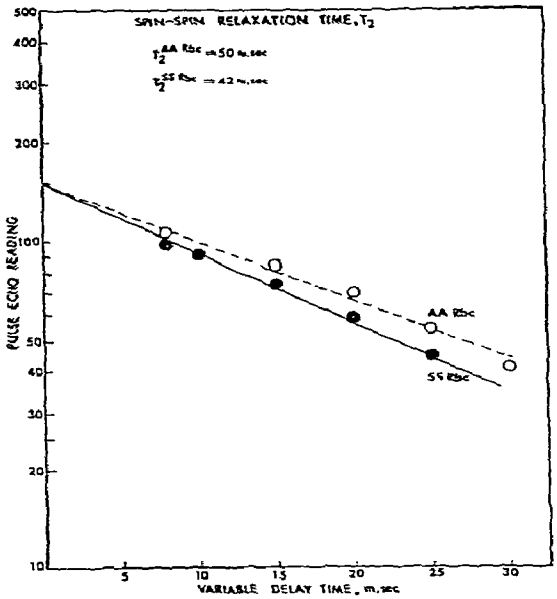

Fig. 9. The spin–spin relaxation time, T_2, of normal AA and sickling SS red blood cells in 0.9% NaCl in H_2O.

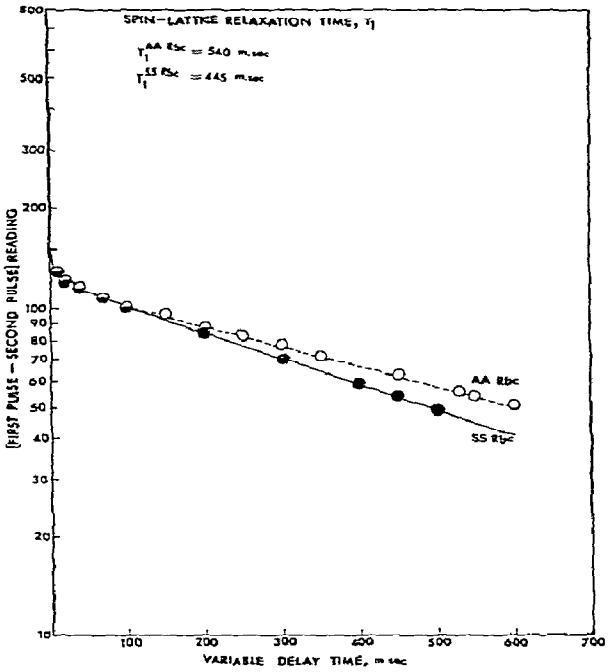

Fig. 10. The spin–lattice relaxation time, T_1, of normal AA and sickling SS red blood cells in 0.9% NaCl in H_2O.

Stern plane as a result of electrostatic or hydrophobic bonding or intercalation into the red blood cell membrane, causing a relocalization of the surface charge density distribution or perturbation of the Stern layer. This phenomenon we have designated as "esotropic" interaction, to differentiate it from "exotropic" interaction in which there is little alteration of the Stern layer.

The variation of K_{app}^{ex} as a function of the thickness of the electrical double layer which we have observed indicates that the binding affinity of polyamines to the normal red blood cell is approximately 30 times greater than to the sickling erythrocyte. This is consistent with our earlier reported findings that the polyamine content of the sickling red blood cell is five to six times that of the normal erythrocyte,

Fig. 11. Fluorescein–spermidine labelling of the normal red blood cell. Photograph was taken using fluorescence microscope (Leitz-Wetzlar ph2, Neofluar 40/0.75).

effectively limiting any further binding with polyamines.

The interaction of polyamines with the red blood cell, therefore, results in specific alteration of the Stern layer which varies in the normal and sickling erythrocyte. These alterations may be attributed to several electrokinetic factors, among them adsorption density (mole/cm^2), coulombic interaction in the electrical double layer, and the contribution of the cohesive potential (or energy) of the ligand to the surface potential of the red blood cell. Based on our studies of the binding isotherms of polyamine with the sickling red blood cell, we found 2.7 to 3.4×10^6 polyamine molecules to be bound at the surface of a single sickling red blood cell. Assuming 10×10^6 molecules of sialic acid are present in the sickling red blood cell membrane surface, the electrostatic interaction between polyamines and sialic acid must be assumed to be quite strong.

Since the nuclear spin relaxation time is dependent upon the molecular reorientation time and, consequently, upon the details of molecular diffusion, both the rotational and translational H_2O molecules can affect the magnitude and direction of the internuclear vector for nuclei in different molecules in a surrounding liquid and, thus, cause fluctuations in the interaction energy between the various magnetic fields (or dipoles). These fluctuations lead to a dipole–dipole spin–lattice relaxation, spin-coupling, and other interactions. The intensity and magnitude of these interaction energies which couples the nuclear precession frequency to the molecular motion, have been used previously to explain the differences observed in T_1 and T_2 for normal versus sickling red blood cells [34,35].

From our examination of the spin–spin relaxation time, T_2, it appears that the proton–proton interaction of water in a solution of packed normal and sickling red blood cells is similar. A difference of approximately 100 ms was, however, observed in the spin–lattice relaxation times of the two types of erythrocytes. Since all the NMR measurements were made on cells which contained oxy-Hb, any differences in T_1 cannot be explained on the basis of aggregation of hemoglobin tetramers. We believe that the observed differences in T_1 may be due to differences at the surface of the red blood cell membrane, rather than at the surface of the hemoglobin molecule.

We have previously reported the presence of polyamines on the sickling red blood cell membrane, resulting in a reduction in the surface charge potential (ψ_0) of 13% over that of the normal erythrocyte [30,32]. The polyamines result in a greater adhesion at the membrane surface and increased hydrophobicity in the sickling red blood cell, as measured by the apparent interfacial viscosity [30]. This suggests that the sickling red blood cell would be much less flexible than the normal erythrocyte.

There is evidence that in proteins the most strongly bound water is hydrogen bonded to the polar side chains, and not to the peptide linkages [41]. Extension of this concept to red blood cell membranes would result in including interactions with the phosphate groups of the phospholipids. The binding of the positively charged polyamines to the negatively charged surface of the cell membrane results not only in a decrease in the surface charge, but also in the replacement of a potential oxygen hydrogen bonding site with a nitrogen hydrogen bonding site. Since chemical exchange can occur between these bonding sites and water, the more nitrogen sites, rather than oxygen, the faster the relaxation. This is true because nitrogen, unlike oxygen, has a nuclear electric quadrupole moment, since for ^{14}N the nuclear spin, I, is equal to 1. This gives rise to a fluctuating magnetic field, the result of which on the relaxation of the water would be expected to decrease T_1 for the sickling erythrocyte, as we have observed.

In speculating on the causes of the elevated blood levels of polyamines which we have found in individuals with sickle cell anemia, the evidence suggests that there may be several contributing factors. Primarily, it would appear that the chronic reticulocytosis characteristic of this desease may result in intercalation of polyamines into the membrane of the immature erythrocytes.

Another possibility which must be considered further is the covalent binding of polyamines at the membrane surface. It is also possible that some equilibration takes place between the polyamines of the leukocytes or granulocytes and the immature red blood cells, which would seem to be supported by the characteristic hemolysis of the sickling erythrocytes. The extent to which any or all of these factors contribute to the accumulation of polyamines in the sickling red blood cell remains to be determined.

References

[1] J.N. Mehaishi, and G.V.F. Seaman, Biochim. Biophys. Acta 112 (1966) 154.
[2] D.A. Haydon, Biochim. Biophys. Acta 50 (1964) 450.
[3] G.V.F. Seaman, in: The red blood cell, Vol. 2, ed. D. MacN. Surgenor (Academic Press, New York, 1975), ch. 27, pp. 1135–1229.
[4] D.E. Brooks, J.S. Millar, G.V.F. Seaman and P.S.J. Vassar, Cell Physiol. 69 (1967) 155.
[5] G.V.F. Seaman and B.A. Pethica, Biochem. J. 90 (1964) 573.
[6] G.V.F. Seaman and G. Uhlenbruck, Arch. Biochem. Biophys. 100 (1963) 493.
[7] R. Roscoe, Brit. J. Appl. Phys. 9 (1952) 280.
[8] H.C. Brinkman, J. Chem. Phys. 20 (1952) 571.
[9] L. Dintenfass, in: Blood microrheology and viscosity factors in blood flow: ischaemia and thrombosis (Appleton, New York, 1971).
[10] S. Chien, S. Usami, R.J. Dillenback and M.I. Gregersen, Am. J. Physiol. 219 (1970) 136.
[11] S. Chien, in: The red blood cell, 2nd Ed., ed. D. MacN. Surgenor (Academic Press, New York, 1975), p. 1031.
[12] T.W. Tillack, R.E. Scott and V.T. Marchesi, J. Exp. Med. 135 (1972) 1209.
[13] R.L. Jackson, J.P. Segrest, I. Kahane and V.T. Marchesi, Biochemistry 12 (1973) 3131.
[14] V.T. Marchesi, T.W. Tillack, R.L. Jackson, J. Segrest and R.E. Scott, Proc. Natl. Acad. Sci. US 69 (1973) 1445.
[15] M. Bessis, in: Living blood cells and their ultrastructure, translated by R.I. Weed (Springer, Berlin, 1973).
[16] B. Larsen, Nature 258 (1975) 345.
[17] J.A. Gordon and M.D. Marquardt, Nature 258 (1975) 346.
[18] E.J.W. Verwey and J.Th.G. Overbeek, in: Theory of the stability of lyophobic colloids, (Elsevier, Amsterdam, 1948).
[19] B.V. Derjoquin, and L.D. Landau, Acta Phys. Chem. USSR 14 (1941) 633.
[20] D.H. Heard and G.V.F. Seaman, J. Gen. Physiol. 43 (1960) 635.
[21] C.W. Tabor and H. Tabor, Ann. Rev. Biochem. 45 (1976) ...
[22] H. Tabor and C.W. Tabor, Pharm. Rev. 16 (1964) 245.
[23] S.S. Cohen, in: Introduction to the polyamines (Prentice Hall, Engelwood Cliffs, 1971).
[24] U. Bachrach, in: Function of naturally occurring polyamines (Academic Press, New York, 1973).
[25] D.H. Russell, ed., in: Polyamines in normal and neoplastic growth (Raven Press, New York, 1973).
[26] D. Lungreen, P. Farrel and P. DiSant'agnese, Cli. Chem. Acta 62 (1975) 357.
[27] O. Rennert, J. Frias and D. laPointe, in: Fundamental Problems of cystic fibrosis and related diseases, eds. J. Mangos and R. Talamo (IMB, 1973) pp. 44–52.
[28] N. Seiler, in: Polyamines in normal and neoplastic growth, ed. D.H. Russeel (Raven Press, New York, 1973).
[29] P.W. Chun, O.M. Rennert, E.E. Faffen, and W. Taylor, J. Biochem. Biophys. Res. Commun. 69 (1976) 1095.
[30] P.W. Chun, S.Y. Shiao, E.E. Saffen, D.O. Shah, W.J. Taylor and R.J. DiTore, Anal. Biochem. (1976).
[31] P.W. Chun, O.M. Rennert, E.E. Saffen, R.J. DiTore, J.B. Shukla, W.J. Taylor and D.O. Shah, in: Recent advances in colloid and surface sciences (1976) to be published.
[32] P.W. Chun, O.M. Rennert, E.E. Saffen and W.J. Taylor, Fed. Proc. 35 abst. 392 (1976) 1432.
[33] T.R. Lindstrom, S.H. Koenig, T. Boussios and J.F. Bertles, Biophys. J. 16 (1976) 679.
[34] A.H. Chuang, M.R. Waterman, K. Yamaoka and G.L. Cottam, Arch. Biochem. Biophys. 167 (1975) 145.
[35] A. Zipp, T.L. James, I.D. Kuntz and S.B. Shohet, Biochim. Biophys. Acta 428 (1976) 291.
[36] A. Zipp, I.D. Kuntz, S.J. Rehfeld and S.B. Shohet, FEBS Letters 43 (1974) 9.
[37] G.L. Cottam, K.M. Valentine, K. Yamaoka and M.R. Waterman, Arch. Biochem. Biophys. 162 (1974) 487.
[38] F. Bloch, W.W. Hansen and M. Pacard, Phys. Rev. 69 (1946) 127.
[39] E.L. Hahn, Phys. Rev. 80 (1950) 580.
[40] A. Katchalsky, E.R. Unanue and M.J. Levinthal, Expt. Med. 136 (1972) 907.
[41] L. Pauling, J. Am. Chem. Soc. 67 (1945) 555.